Bioorganic & Medicinal Chemistry xxx (2018) xxx–xxx

Contents lists available at ScienceDirect

Bioorganic & Medicinal Chemistry

journal homepage: www.elsevier.com/locate/bmc

Novel oxazolxanthone derivatives as a new type of α-glucosidase inhibitor: synthesis, activities, inhibitory modes and synergetic effect

Sen-Miao Ding, Tian Lan, Gao-Jie Ye, Jia-Jun Huang, You Hu, Yi-Ran Zhu, Bo Wang *

School of Chemistry, Sun Yat-sen University, 135 Xingang West Road, Guangzhou 510275, PR China

ARTICLE INFO

Article history:
Received 20 March 2018
Revised 3 May 2018
Accepted 5 May 2018
Available online xxxx

Keywords:
Oxazolxanthones
α-Glucosidase inhibitors
Docking
Synergetic effect
Non-competitive and competitive

ABSTRACT

Xanthone derivatives have shown good α-glucosidase inhibitory activity and have drawn increased attention as potential anti-diabetic compounds. In this study, a series of novel oxazolxanthones were designed, synthesized, and investigated as α-glucosidase inhibitors. Inhibition assays indicated that compounds **4**–**21** bearing oxazole rings exhibited up to 30-fold greater inhibitory activity compared to their corresponding parent compound **1b**. Among them, compounds **5**–**21** (IC_{50} = 6.3 ± 0.4–38.5 ± 4.6 μM) were more active than 1-deoxynojirimycin (IC_{50} = 60.2 ± 6.2 μM), a well-known α-glucosidase inhibitor. In addition, the kinetics of enzyme inhibition measured by using Lineweaver–Burk analysis shows that compound **4** is a competitive inhibitor, while compounds **15**, **16** and **20** are non-competitive inhibitors. Molecular docking studies showed that compound **4** bound to the active site pocket of the enzyme while compounds **15**, **16**, and **20** did not. More interestingly, docking simulations reveal that some of the oxazolxanthone derivatives bind to different sites in the enzyme. This prediction was further confirmed by the synergetic inhibition experiment, and the combination of representative compounds **16** and **20** at the optimal ratio of 4:6 led to an IC_{50} value of 1.9 ± 0.7 μM, better than the IC_{50} value of 7.1 ± 0.9 μM for compound **16** and 8.6 ± 0.9 μM for compound **20**.

1. Introduction

α-Glucosidase (EC 3.2.1.20) is an enzyme which catalyzes the hydrolysis of glycosidic bonds in complex carbohydrates, playing a key role in the digestion of dietary carbohydrates and in the processing of glycoproteins and glycolipids. Inhibitors of α-glucosidase can delay carbohydrate digestion and prolong the overall carbohydrate digestion time, thereby helping to reduce elevated blood sugar levels after a meal.[1–4] Amongst the α-glucosidase inhibitors, acarbose, miglitol, and voglibose have being used as first-line treatments for type 2 diabetes in the clinical setting.[5–7] Moreover, α-glucosidase inhibitors have become important therapies in viral infections, including HIV and influenza, and also have therapeutic potential in metastatic cancer, obesity, and lysosomal storage diseases.[8–11]

The hetero-tricyclic structure of xanthone (**1a**, Chart 1) has been found in a wide variety of natural products bearing various bioactivities.[12,13] In previous studies, we have shown that xanthone derivatives could act as α-glucosidase inhibitors.[14–18] We have found that the derivatives bearing hydroxyl groups (e.g., **1b**) or extended π-conjugated systems (e.g., **1c**), exhibit greater inhibitory effects than compound **1a**. Our investigations suggested that the 3-hydroxyl group of **1b** may not be required for the inhibitory activity because the 3-arylacyloxyxanthone derivative **1d** shows greater inhibitory effects than **1b.**[19] This finding also implies that the addition of aromatic moieties by esterification at the 3-OH of **1b** is an effective strategy to increase the inhibition activity. However, as oral therapies for diabetes, ester-bearing compounds may have considerable limitations because of their susceptibility to hydrolysis by intestinal esterases.

In response to these issues, we have been keenly interested in investigating modifications of the 3-OH that may bring about improved stability and higher bioactivity. Previously, our quantitative structure-activity relationship (QSAR) study on xanthone derivatives found that the number of H-bonds formed, the number of aromatic rings and the chemical softness value are positively correlated with the inhibitory effect.[16] This finding suggests that adding heteroaromatic rings can bring additional π-systems and heteroatoms as H-bond donors/acceptors, and which improve the chemical softness, might be a good way to enhance both the stability and the bioactivity. Among the various heteroaromatic rings, oxazole rings have particularly drawn our attention, thanks to their unique properties as key building blocks for compounds having various bioactivity, including anti-inflammatory,[20] antibacterial,[21]

* Corresponding author.
E-mail address: ceswb@mail.sysu.edu.cn (B. Wang).

https://doi.org/10.1016/j.bmc.2018.05.008
0968-0896/

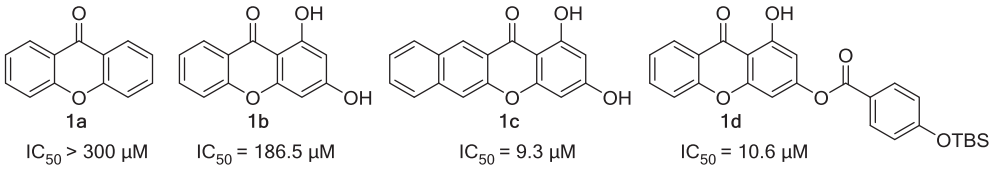

Chart 1. Structures of xanthone derivatives **1a–d.**

antifungal[22] antiproliferative,[23] anti-tuberculosis,[24] muscle relaxant,[25] HIV inhibitory[26] and hypoglycemic activity.[27]

With these considerations in mind, we designed and synthesized a series of oxazole-containing xanthone derivatives **4–18** (Scheme 1) with the aim to clarify the role of the oxazole ring in the inhibition of α-glucosidase. We also synthesized compounds **19–21** in order to clarify the necessity of the 5-OH group in compounds **4–18** and to gain further insight into the structure–activity relationship of oxazolxanthone derivatives as α-glucosidase inhibitors. We conducted a series of inhibition assays and kinetic assays to characterize the inhibitory activities of these compounds, and we also investigated the potential for synergistic inhibition. Additionally, we carried out molecular docking studies to gain insight into possible modes of binding with α-glucosidase.

2. Results and discussion

2.1. Synthesis of xanthone derivatives 1b and 2-21

The synthetic route of xanthone derivatives **1b** and **2–21** is shown in Scheme 1. Compound **1b** was synthesized from the condensation of hydroxybenzoic acid with phloroglucinol in the presence of anhydrous zinc chloride and phosphoryl chloride.[28,29] Compound **2** was obtained from the nitration of compound **1b** with 70% HNO_3 in acetic acid,[30,31] and then was hydrogenated in acetone with Pd/C as catalyst to produce compound **3**. Compounds **4–16** were obtained in 33–59% yields by heating the appropriate acid with compound **3** in Eaton's reagent (7.5% W/W P_2O_5). Demethylation of compound **16** in CH_2Cl_2 with BBr_3 gave compound **17**. Hydrogenation of compound **8** in acetone with Pd/C as catalyst produced compound **18**. Compounds **19–21** were prepared in 88–92% yields from the methylation of compounds **6, 11** and **16**, respectively, with CH_3I in the presence of K_2CO_3 under reflux.[32,33] Compounds **1b** and **2–21** were characterized by HRMS (EI or ESI) and NMR (^1H and ^{13}C). HMQC and HMBC were also performed to determine the chemical structure of compound **2**.

2.2. Determination of the structure of compound 2

Under the nitration condition, both hydrogen atoms (H-2 and H-4) of compound **1b** are able to be substituted. Therefore it was necessary to determine the structure of the intermediate product (compound **2**) by 2D-NMR (HMQC and HMBC). In the ^1H NMR spectrum of compound **1b** (Fig. S1), two aromatic protons H-2 and H-4 were observed at 6.41 and 6.22 ppm, respectively, as doublets due to their long-distance coupling of 2.1 Hz. However, in the range of 6–7 ppm, only one singlet was observed at 6.37 ppm for compound **2** (Fig. S5). This indicated that the nitro group was installed on the xanthone skeleton at either the C-2 or C-4 positions. The exact position was determined using HMBC and HMQC.

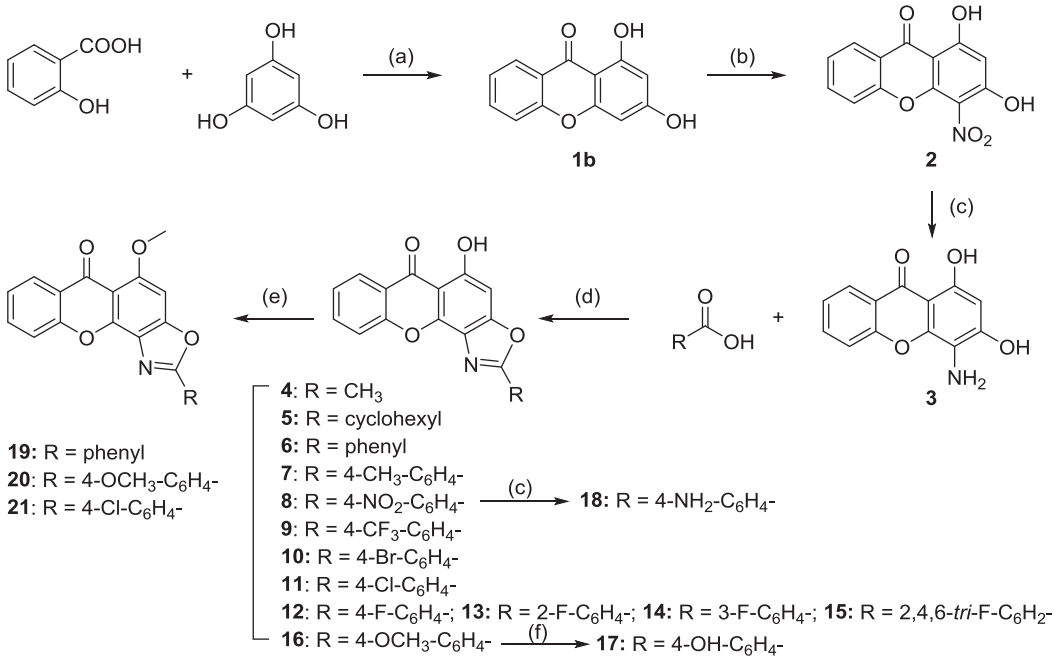

Reagents and conditions: **(a)** $ZnCl_2$, $POCl_3$, 75 °C, 2.5h, 79% yield; **(b)** HNO_3, CH_3COOH, 50 °C, 2h, 59% yield; **(c)** H_2, Pd/C, 40 °C, 12h, 90%, 86% yield; **(d)** Eaton's reagent, 110 °C, 3h, 33%-59% yield; **(e)** CH_3I, K_2CO_3, r.t., 24h, 88%-92% yield; (f) BBr_3, N_2,-8 °C-r.t., 81% yield.

Scheme 1. Synthesis of compounds **1b**, **2–21**.

As can be seen from HMBC (Fig. S7), a sharp singlet was observed at 13.07 ppm that was assignable to the chelated 1-OH group. This 1-OH showed strong correlations with the carbon signals at 163.8, 101.7 and 98.4 ppm. On the other hand, HMQC (Fig. S8) indicated that hydrogen signals at 6.37 ppm showed strong correlations with the carbon signals at 98.4 ppm. These results indicated that the H-2 was preserved and H-4 was substituted by a nitro group.

2.3. α-Glucosidase inhibitory activity

The inhibitory activities of compounds **1b** and **2**–**21** in yeast α-glucosidase were evaluated by method described previously.[14–19] The IC_{50} values obtained, along with those of compounds **1b, 2,** and **3**, as well as 1-deoxynojirimycin as a positive control for comparison are shown in Table 1. Some structure–activity relationships may be derived from examination of the IC_{50}values of compounds **4**–**21**.

Table 1
In vitro α-glucosidase inhibitory activity of compounds **1b, 2–21.**

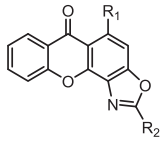

Compound	R_1	R_2	IC $_{50}$ (μM)
1b			186.5 ± 12.4
2			286.4 ± 10.5
3			126.6 ± 9.3
4	OH	H	64.4 ± 5.0
5	OH		38.5 ± 4.6
6	OH		18.3 ± 0.7
7	OH	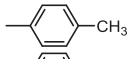	19.1 ± 1.5
8	OH	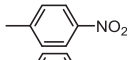	24.5 ± 5.1
9	OH	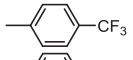	26.9 ± 3.8
10	OH	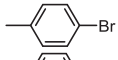	11.0 ± 1.1
11	OH	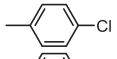	8.8 ± 0.6
12	OH	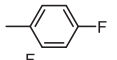	6.7 ± 1.2
13	OH		8.4 ± 0.6
14	OH		8.9 ± 0.5
15	OH	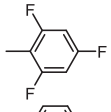	6.3 ± 0.4
16	OH	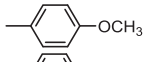	7.1 ± 0.9
17	OH	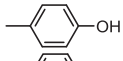	7.3 ± 0.9
18	OH	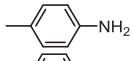	8.3 ± 1.8
19	OCH_3		19.6 ± 0.6
20	OCH_3	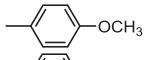	8.6 ± 0.9
21	OCH_3	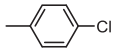	9.9 ± 0.2
1-deoxynojirimycin			60.3 ± 6.2

The first observation is that the weak inhibitory activity of xanthones can be amplified by inserting one oxazole ring. As can be seen, the inhibitory activity of compound **4,** which has one conjugated oxazole ring, was increased by about 3-fold compared to compound **1b**, 4.5-fold compared to compound **2**, and 2-fold compared to compound **3**.

More significantly, compound **5**, which has one cyclohexyl group attached to the oxazole ring, showed higher activity, and compounds **6** and **7,** with one more benzene ring attached to the oxazole ring, were much more active than compound **4** and even more active than 1-deoxynojirimycin, a well-known α-glucosidase inhibitor. These results suggest that the addition of either a cyclohexyl or a benzene ring may enhance the interaction of these compounds with the enzyme through the hydrophobic or π-stacking effect. Compounds **8** and **9**, which bear electron-withdrawing substituents such as the nitryl or trifluoromethyl groups on the linked benzene ring, showed decreased inhibitory activity compared to compounds **6** and **7,** while compounds **16**, **17** and **18**, which have electron donating groups such as the methoxy, hydroxyl and amino groups, showed significantly greater inhibitory activity.

Furthermore, the introduction of various halogen groups at the linked benzene ring (compounds **10**–**15**) increased the inhibitory activity. And the increase in inhibitory activity was not affected by the number of halogens or their positions of substitution. Compound **15** showed the highest inhibitory activity, with an IC_{50} value of 6.3 ± 0.4 μM, a nearly 30-fold increase compared to compound **1b**.

In order to further clarify the role of the 5-OH group in compounds **4**–**21**, compounds **6, 11** and **16** were methylated to produce compounds **19**–**21**, respectively. Comparison of the inhibitory activity of compounds **6, 11** and **16** with **19**–**21** showed that the corresponding 5-OH or 5-OMe derivatives possess similar IC_{50}, suggesting that the H-bond donor effect might be the most possible interaction between these groups and the enzyme. An interesting observation is that compounds **19**–**21** showed better solubility than the corresponding compounds having a 5-OH, for which solubility may be negatively impacted by an intramolecular H-bond. This observation provides important insights for the further design of new α-glucosidase inhibitors using the skeleton of oxazolxanthone.

2.4. Inhibition kinetics of α–glucosidase

In order to gain further insight into how these xanthone derivatives interact with yeast α-glucosidase, the mode of inhibition for compounds **4**, **15, 16** and **20** as representative examples were determined from Lineweaver-Burk plots using the methods described previously.[34,35] The double reciprocal plots are shown in Fig. 1. As can be seen, the double reciprocal plot of compound **4** showed straight lines with the same V_{max}, which indicates that compound **4** is a competitive inhibitor of α-glucosidase, while the double reciprocal plots of compounds **15, 16** and **20** showed straight lines with the same Michaelis constant (K_m), suggesting that compounds **15**, **16** and **20** are non-competitive inhibitors of α-glucosidase. The inhibition constants (K_i) were 6.8 μM for compound **15** (6 μM), 5.3 μM for compound **16** (5 μM) and 7.4 μM for compound **20** (7 μM), respectively.

2.5. Molecular docking studies

To gain further insights into the binding mode of these oxazolxanthone derivatives, molecular docking studies were performed.

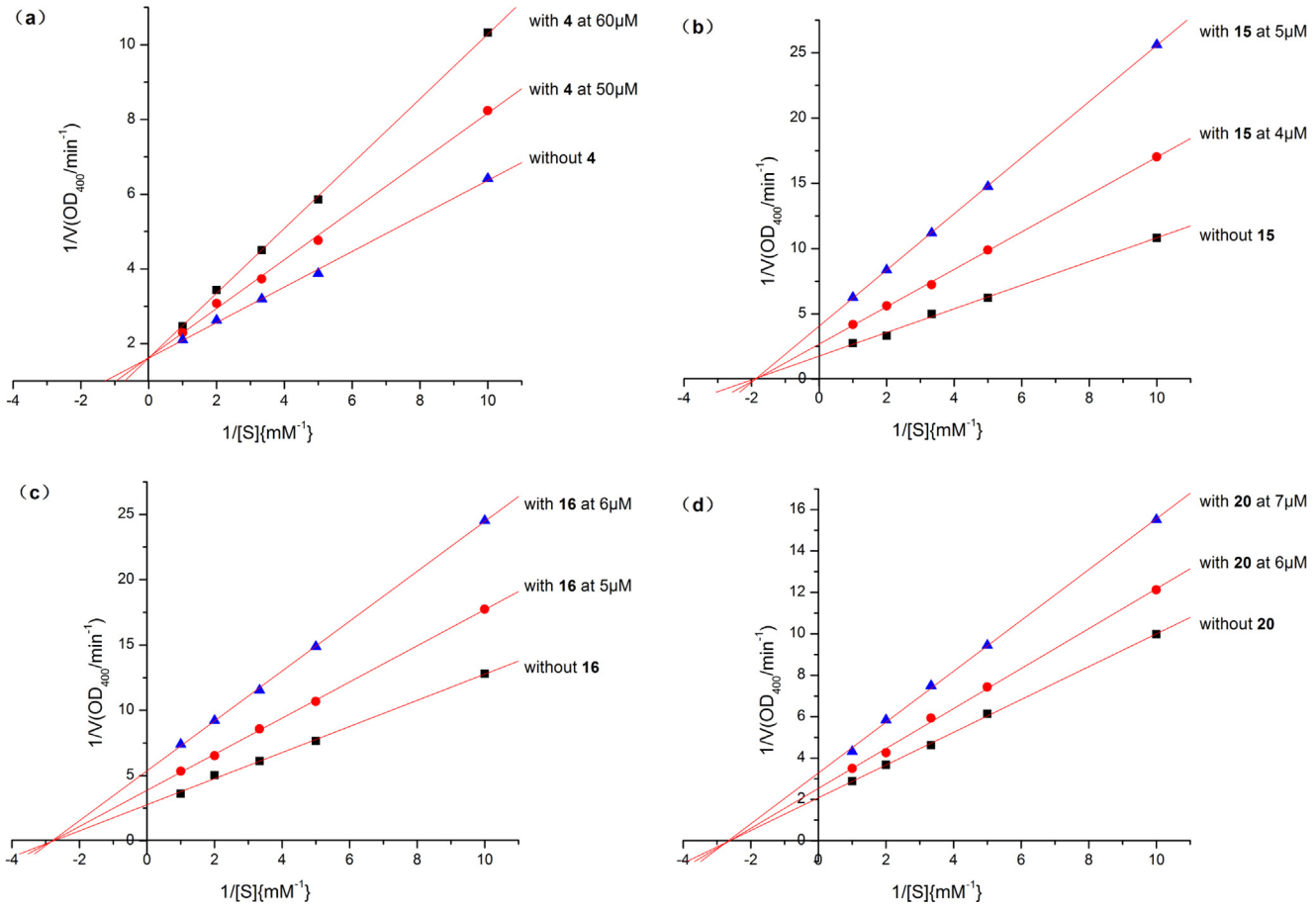

Fig. 1. Double-reciprocal plots of the inhibition kinetics of yeast α–glucosidase by compounds **4** (a), **15** (b), **16** (c) and **20** (d).

From the structure-activity relationships discussed above, we were particularly interested in the effect of the oxazole ring and the additional phenyl groups. Therefore, compounds **15, 16**, **18**, **20** and **21**, which are among the most efficient inhibitors, were chosen for the docking simulations. Compounds **4**, **6** and the parent compound **1b** were also studied for comparison.

Since the X-ray crystal structure of α-glucosidase from *Saccharomyces cerevisiae* is currently unavailable, the homology modeling provided by SWISS-MODEL Repository, with the model quality estimation performed,[36] was used as the receptor. From the docking studies, the binding affinity of oxazolxanthone **4** was predicted to be −33.07 kJ·mol^{-1}, greater than the parent compound **1b** (−32.65 kJ·mol^{-1}). Also, when a phenyl group was added to the oxazole ring, as in compounds **6** (−39.76 kJ·mol^{-1}), **15** (−42.70 kJ·mol^{-1}), **16** (−41.02 kJ·mol^{-1}), **18** (−40.60 kJ·mol^{-1}), **20** (−38.51 kJ·mol^{-1}) and **21** (−40.18 kJ·mol^{-1}), the binding affinity was further increased. This suggests that introducing an oxazole ring into the core structure of xanthone could lead to stronger binding with α-glucosidase, and an additional phenyl group attached to the oxazole ring could further improve the interaction with the enzyme, which is consistent with the observations in the enzyme inhibitory essays.

Molecular docking analysis suggests that several types of interactions are formed between the inhibitor and the enzyme upon binding, as seen in Fig. 2, the heteroatoms in the oxazole ring can form hydrogen bonds with specific residues in the protein. Additionally, both the core structure of the oxazolxanthones and the additional phenyl group can participate in the formation of π-π interactions. Moreover, π-cation interactions may also exist as a noncovalent intermolecular force between the additional phenyl groups of some of these compounds and ionized residues such as lysine.

As shown in Fig. 3, molecular docking analysis suggests that compound **4** has a possible binding position close to the active site of α-glucosidase (Asp214, Glu276 and Asp349), while the other six docked compounds all bind to allosteric sites in the enzyme, which is consistent with the results from the enzyme kinetic assay demonstrating that compound **4** is a competitive inhibitor and the other compounds are noncompetitive inhibitors. Another interesting result we observed, also shown in Fig. 3, is that compounds **20** and **21** with a methoxy group on the 5-position bind to a different position on the enzyme compared to those having an hydroxy group on the 5-position, i.e. compounds **6**, **15**, **16** and **18**. Taken together, this suggests the presence of multiple binding modes for these inhibitors of α-glucosidase.

2.6. Synergetic inhibition

We previously reported that the inhibitors 1, 3, 7-trihydroxyxanthone and 1, 3-dihydroxybenzoxanthone interacted with the enzyme in multiple binding configurations, thus having a synergetic effect.[18] The observation that compounds **20** and **21** may have different binding modes from compounds **6**, **15**, **16**, and **18** suggested that they may also exhibit such synergetic inhibitory effect when used in combination. Therefore, we decided to perform synergetic inhibition assays.

Compounds **16** and **20**, possessing greater inhibitory activity and minimal structural differences, were selected for investigation of synergetic inhibition. We investigated their inhibitory effect individually and in combination in varying molar ratios as

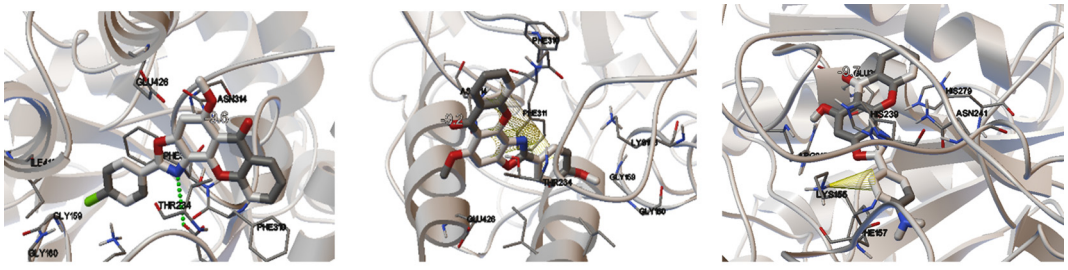

Fig. 2. Predicted interactions between α-glucosidase and compounds **21** (a), **20** (b) and **18** (c).

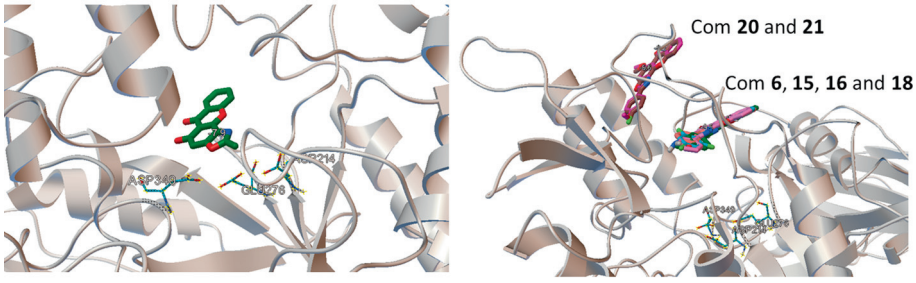

Fig. 3. Binding positions of compound **4** (a) and compounds **6**, **15**, **16**, **18**, **20** and **21** (b).

previously described.[18,34,35,37] As shown in Fig. 4, compounds **16** (2 μM) and **20** (2 μM) inhibited the enzyme by 21.7% and 20.3%, respectively. However, when applied together in a 1:1 M ratio (2 μM total), the enzyme was inhibited by 41.9%, a 2-fold increase. This result suggests that the combination of compounds **16** and **20** indeed produces synergetic inhibition.

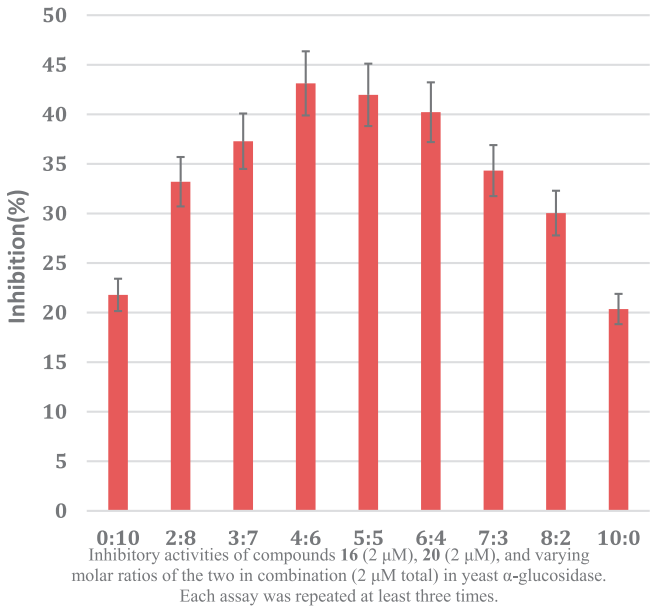

Fig. 4. Inhibitory activities of compounds **16**, **20** and varying combinations of the two.

Further assays were performed to determine the optimal ratio of compound **16** to compound **20**. A series of mixtures of compounds **16** and **20** with fixed total concentrations (2 μM) but varying molar ratios were prepared, and inhibition assays were carried out. As shown in Fig. 4, the optimal molar ratio of compound **16** to compound **20** was found to be 4:6.

We then measured the IC_{50} value of the two inhibitors together at this optimal ratio and obtained an IC_{50} value of 1.9 ± 0.3 μM, which is 3.5- and 4-fold better than those of compound **16** (IC_{50} = 7.1 ± 0.9 μM) and compound **20** (IC_{50} = 8.6 ± 0.9 μM) alone, respectively. These observations not only confirm the synergetic inhibition of the two compounds but also suggest that they interact with the enzyme via different modes of binding, as observed in the molecular docking studies.

3. Conclusions

In summary, a series of novel oxazolxanthone derivatives have been synthesized, and their inhibitory activities against α-glucosidase were evaluated. The results indicate that oxazolxanthones display potent inhibition of α-glucosidase. The structure–activity relationship analysis suggests that the introduction of an oxazole ring, as well as additional phenyl groups attached to the oxazole ring, can enhance inhibitory activity. Addition of electron donating groups and halogens to the additional phenyl ring can further enhance the inhibitory activity, while the addition of electron withdrawing groups reduce the inhibitory activity. Compound **15** shows the highest inhibitory activity, nearly 30-fold more than compound **1b**. Lineweaver–Burk analysis revealed that the representative oxazolxanthones **15**, **16** and **20** inhibit α–glucosidase via a non-competitive mechanism, while compound **4** inhibits α–

glucosidase via a competitive mechanism. Docking studies showed that hydrogen bonding interactions with the oxazole ring, π stacking interactions with oxazolxanthone, and π-cation interactions involving the additional phenyl group play a crucial role in mediating the inhibitory effect. In addition, the prediction of multiple binding modes by molecular docking studies was verified by the observation of synergetic inhibition involving compounds **16** and **20** in α-glucosidase, suggesting that the two inhibitors may bind simultaneously to the enzyme in different allosteric locations to generate good synergetic inhibition of enzyme activity.

4. Experimental and methods

4.1. General information

Melting points were determined using a SGW X-4 digital melting point apparatus, and the temperatures were not corrected. High resolution (HR) mass spectra were measured on an LTQ Orbitrap Elite or TSQ Quantum XLS mass spectrometer. IR spectra were measured on a Bruker EQUINOX55 Fourier transformation infrared spectrometer with KBr pellets. The NMR (^{1}H, ^{13}C, HMQC and HMBC) were recorded on Bruker AVANCE 400, Varian INOVA 500NB and Bruker Avance III 600 instruments in $CDCl_3$, DMSO-d_6 or a solvent mixture of $CDCl_3$/CF_3COOD with tetramethylsilane (TMS) as an internal standard. UV spectra were recorded on a Shimadzu UV-3250 scanning spectrophotometer.

1-Deoxynojirimycin, *p*-nitrophenyl (PNP)-α-D-glucopyranoside, and α-glucosidase (from *Saccharomyces cerevisiae*) were purchased from Sigma (St. Louis, MO, USA). Other reagents and solvents were purchased from commercial sources and used without further purification. Analytical thin layer chromatography was performed on pre-coated silica gel (GF-254), and column chromatographic purifications were performed using 300–400 mesh silica gel. Spots were visualized under ultraviolet light at 254 and 366 nm.

Compound **1b** was prepared as previously reported.[17]

4.2. Synthesis of 1, 3-dihydroxy-4-nitro-9H-xanthen-9-one (*2*)

Nitric acid (70%, 1.0 mL) in acetic acid (5.0 mL) was slowly added to a solution of compound **1b** (20.0 mmol) in acetic acid (20.0 mL). The mixture was stirred at 50 °C for 2.0 h and then poured into ice-cooled water (200 mL). The formed precipitates were filtered, washed with water. The crude products was purified by flash chromatography (EtOAc/petroleum ether, 1:3) to yield compound **2** (3.2 g, 58.6%) as a yellow solid. Mp 226–228 °C; IR (KBr): 3346, 3277, 2920, 1662, 1611, 1519, 1465, 1392, 1339, 1285, 1194, 938, 899, 753, 701, 643 cm^{-1}; ^{1}H NMR (600 MHz, DMSO-d_6) δ 13.04 (s, 1H), 8.15 (dd, *J* = 7.9, 1.7 Hz, 1H), 7.89 (ddd, *J* = 8.6, 7.1, 1.7 Hz, 1H), 7.61 (dd, *J* = 8.5, 0.9 Hz, 1H), 7.54 (ddd, *J* = 8.0, 7.2, 1.0 Hz, 1H), 6.37 (s, 1H). ^{13}C NMR (151 MHz, DMSO-d_6) δ 180.04, 163.78, 158.73, 155.18, 149.91, 136.82, 125.98, 125.82, 122.52, 120.24, 118.35, 101.75, 98.35. HRMS (ESI) calcd for $C_{13}H_6O_6N$ [M−H]$^-$:272.0200 found 272.0201.

4.3. Synthesis of 1, 3-dihydroxy-4-amino-9H-xanthen-9-one(*3*)

To a solution of **2** (2.7 g,) in acetone (200 mL) Pd-C (0.3 g) was added as catalyst and hydrogenation was carried out at 1 bar for 12 h at 40 °C. The resulting suspension was filtered and concentrated under reduced pressure to get crude products which were recrystallized from ethyl acetate to yield pure products **3** (2.2 g, 90.5%). Mp 196–197 °C; IR (KBr): 3081, 2921, 2851, 1659, 1610, 1576, 1532, 1470, 1350, 1284, 1257, 1219, 1142, 999, 975, 868, 812, 763, 743, 703, 666, 610 cm^{-1}; ^{1}H NMR (400 MHz, DMSO-d_6) δ 12.13 (s, 1H), 8.11 (d, *J* = 8.0 Hz, 1H), 7.83 (t, *J* = 7.9 Hz, 1H), 7.61 (d, *J* = 8.4 Hz, 1H), 7.43 (t, *J* = 7.4 Hz, 1H), 6.29 (s, 1H); ^{13}C NMR (101 MHz, DMSO-d_6) δ 180.58, 156.00, 153.62, 142.99, 135.90, 125.72, 124.61, 124.46, 120.07, 118.23, 116.56, 102.40, 97.83; HRMS (ESI) calcd for $C_{13}H_8NO_4$ [M−H]$^-$: 242.0453 found 242.0456.

4.4. General procedure for the preparation of compounds *4–16*

The derivatives were synthesized by heating compound **3** (1.0 mmol) with suitable acid (1.2 mmol) in Eaton's reagent (7.5% W/W P_2O_5, 24.0 g) and stirring at 100–120 °C for 3 h. At the end of the reaction period, the residue was poured into an ice-water mixture and neutralized with an excess of NaOH (10%) solution, and the residue was filtered and dissolved in chloroform. After the evaporation of solvent under vacuum, the crude product was obtained and the residue after evaporation was purified by flash chromatography (chloroform/petroleum ether 10:1) to give compounds **4**–**16**. (33%-59% yield).

4.4.1. 5-hydroxy-2-methyl-6H-xantheno [4, 3-d] oxazol-6-one (*4*)

Yellow solid (57% yield). Mp 234–236 °C; IR (KBr): 3085, 2927, 1657, 1630, 1612, 1577, 1484, 1451, 1388, 1278, 1222, 1132, 1106, 1090, 976, 896, 787, 764, 749, 647 cm^{-1}; ^{1}H NMR (400 MHz, $CDCl_3$) δ 12.99 (s, 1H), 8.34 (dd, *J* = 8.0, 1.7 Hz, 1H), 7.80 (ddd, *J* = 8.7, 7.1, 1.7 Hz, 1H), 7.72–7.65 (m, 1H), 7.52–7.40 (m, 1H), 6.91 (s, 1H), 2.69 (s, 3H); ^{13}C NMR (101 MHz, $CDCl_3$) δ 181.85, 163.25, 160.27, 156.99, 155.68, 146.84, 135.65, 126.11, 124.76, 121.97, 120.78, 118.08, 106.10, 93.39, 14.40; HRMS (ESI) calcd for $C_{15}H_{10}O_4N$ [M+H]$^+$:268.0593 found 268.0603.

4.4.2. 2-cyclohexyl-5-hydroxy-6H-xantheno [4, 3-d] oxazol-6-one (*5*)

Yellow solid (50% yield). Mp 256–258 °C; IR (KBr): 3087, 2921, 2851, 1659, 1610, 1532, 1470, 1449, 1389, 1350, 1285, 1257, 1219, 1189, 1105, 975, 905, 868, 812, 763, 743, 703, 666, 648, 610, 525 cm^{-1}; ^{1}H NMR (400 MHz, $CDCl_3$) δ 13.00 (s, 1H), 8.33 (dd, *J* = 7.9, 1.7 Hz, 1H), 7.79 (ddd, *J* = 8.7, 7.0, 1.7 Hz, 1H), 7.70 (dd, *J* = 8.4, 1.1 Hz, 1H), 7.45 (ddd, *J* = 8.1, 7.0, 1.1 Hz, 1H), 6.91 (s, 1H), 3.00 (tt, *J* = 11.6, 3.6 Hz, 1H), 2.05 (ddt, *J* = 120.8, 13.0, 2.6 Hz, 4H), 1.76 (td, *J* = 11.7, 3.0 Hz, 4H), 1.44 (qt, *J* = 14.1, 2.8 Hz, 2H); ^{13}C NMR (101 MHz, $CDCl_3$) δ 181.86, 169.99, 160.21, 156.74, 155.70, 147.05, 135.55, 126.08, 124.68, 121.83, 120.77, 118.18, 106.04, 93.44, 93.38, 38.03, 30.48(2C), 25.68(2C), 25.62; HRMS (ESI) calcd for $C_{20}H_{16}O_4N$ [M−H]$^-$:334.1084 found 334.1084.

4.4.3. 5-hydroxy-2-phenyl-6H-xantheno [4, 3-d] oxazol-6-one (*6*)

Yellow solid (52% yield). Mp 260–262 °C; IR (KBr): 3072, 2917, 1658, 1611, 1470, 1447, 1391, 1283, 1155, 1098, 1021, 899, 813, 785, 748, 699, 685 cm^{-1}; ^{1}H NMR (400 MHz, $CDCl_3$) δ 13.11 (s, 1H), 8.35 (dd, *J* = 8.0, 1.6 Hz, 1H), 8.28 (dd, *J* = 7.4, 2.2 Hz, 1H), 7.82 (ddd, *J* = 8.6, 7.0, 1.7 Hz, 1H), 7.76 (d, *J* = 8.4 Hz, 1H), 7.55 (dt, *J* = 5.4, 2.4 Hz, 3H), 7.48 (t, *J* = 7.2 Hz, 1H), 7.02 (s, 1H); ^{13}C NMR (101 MHz, $CDCl_3$) δ 181.87, 162.67, 160.78, 156.81, 155.74, 147.45, 135.68, 131.78, 129.01(2C), 127.58(2C), 126.34, 126.14, 124.84, 123.00, 120.85, 118.24, 106.46, 93.59; HRMS (ESI) calcd for $C_{20}H_{12}O_4N$ [M+H]$^+$:330.0760 found 330.0750.

4.4.4. 5-hydroxy-2-(p-tolyl)-6H-xantheno [4, 3-d] oxazol-6-one (*7*)

Yellow solid (55% yield). Mp 263–265 °C; IR (KBr): 3022, 2920, 1655, 1639, 1610, 1471, 1442, 1412, 1385, 1269, 1226, 1184, 1156, 1138, 1047, 1018, 920, 809, 788, 762, 722, 681, 635 cm^{-1}; ^{1}H NMR (400 MHz, $CDCl_3$) δ 13.02 (s, 1H), 8.37 (dd, *J* = 7.8, 1.7 Hz, 1H), 8.17 (d, *J* = 8.2 Hz, 2H), 7.81 (td, *J* = 7.7, 6.9, 1.7 Hz, 1H), 7.75 (d, *J* = 8.6 Hz, 1H), 7.46 (t, *J* = 7.2 Hz, 1H), 7.34 (d, *J* = 8.0 Hz, 2H), 7.00 (s, 1H), 2.46 (s, 3H); ^{13}C NMR (101 MHz, $CDCl_3$/CF_3COOD) δ 182.08, 164.26, 160.96, 155.57, 155.32, 146.07, 145.98, 137.03, 130.51 (2C), 128.27(2C), 126.06, 125.79, 120.18, 119.94, 117.96, 117.90,

106.85, 94.12, 21.80. HRMS (ESI) calcd for $C_{21}H_{12}O_4N$ $[M-H]^-$:342.0771 found 342.0772.

*4.4.5. 5-hydroxy-2-(4-nitrophenyl)-6H-xantheno [4, 3-d] oxazol-6-one (**8**)*

Yellow solid (33% yield). Mp 272–274 °C; IR (KBr): 3083, 2921, 2851, 1695, 1611, 1577, 1532, 1452, 1389, 1351, 1218, 1188, 1157, 1106, 999, 976, 930, 870, 762, 744, 704, 668, 647 cm^{-1}; ^1H NMR (400 MHz, $CDCl_3/CF_3COOD$) δ 8.58–8.49 (m, 4H), 8.40 (dd, J = 8.1, 1.6 Hz, 1H), 8.02 (ddd, J = 8.7, 7.2, 1.7 Hz, 1H), 7.75 (dd, J = 8.6, 1.0 Hz, 1H), 7.66 (ddd, J = 8.1, 7.2, 1.1 Hz, H), 7.26 (s, 1H); ^{13}C NMR (101 MHz, $CDCl_3/CF_3COOD$) δ 186.91, 165.74, 165.17, 160.82, 160.03, 154.14, 151.93, 141.50, 136.27, 134.66, 133.44, 133.11, 130.22, 129.60, 128.96, 125.64, 124.36, 122.28, 111.14, 98.44; HRMS (ESI) calcd for $C_{20}H_9O_6N_2$ $[M-H]^-$:373.0466 found 373.0467.

*4.4.6. 5-hydroxy-2-(4-(trifluoromethyl) phenyl)-6H-xantheno [4,3-d]-oxazol-6-one (**9**)*

Yellow solid (49% yield). Mp 269–270 °C; IR (KBr): 3047, 2961, 2922, 2852, 1936, 1636, 1472, 1452, 1613, 1390, 1324, 1287, 1261, 1220, 1175, 1142, 1114, 1064, 1016, 899, 869, 910, 789, 758, 695, 638, 611 cm^{-1}; ^1H NMR (600 MHz, $CDCl_3$) δ 13.14 (s, 1H), 8.39 (d, J = 8.1 Hz, 2H), 8.35 (dd, J = 7.9, 1.7 Hz, 1H), 7.83 (ddd, J = 8.6, 7.0, 1.7 Hz, 1H), 7.80 (d, J = 8.2 Hz, 2H), 7.75 (dd, J = 8.5, 1.0 Hz, 1H), 7.49 (ddd, J = 8.1, 7.0, 1.1 Hz, 1H), 7.02 (s, 1H); ^{13}C NMR (101 MHz, $CDCl_3/CF_3COOD$) δ 177.04, 157.00, 156.30, 151.44, 150.74, 142.47, 131.67, 129.27 (q, J = 32.9 Hz), 123.24(2C), 121.56 (q, J = 3.8 Hz), 121.30, 120.65, 118.69 (q, J = 272.4 Hz), 116.57, 115.64, 113.19, 101.85, 88.99; HRMS (EI) calcd for $C_{21}H_{10}O_4NF_3$ $[M^+]$: m/z = 397.0556 found 397.0554.

*4.4.7. 2-(4-bromophenyl)-5-hydroxy-6H-xantheno [4, 3-d] oxazol-6-one (**10**)*

Yellow solid (54% yield). Mp 276–278 °C; IR (KBr): 3031, 2918, 1658, 1633, 1610, 1578, 1470, 1403, 1387, 1333, 1283, 1258, 1218, 1097, 1069, 1041, 1008, 975, 900, 829, 779, 766, 751, 723, 682, 648, 613 cm^{-1}; ^1H NMR (500 MHz, $CDCl_3$) δ 13.08 (s, 1H), 8.37 (dd, J = 7.9, 1.7 Hz, 1H), 8.15 (d, J = 8.6 Hz 2H), 7.82 (ddd, J = 8.7, 7.0, 1.7 Hz, 1H), 7.75 (d, J = 8.5 Hz, 1H), 7.68 (d, J = 8.6 Hz, 2H), 7.48 (ddd, J = 8.0, 7.0, 1.1 Hz, 1H), 7.01 (s, 1H); ^{13}C NMR (101 MHz, $CDCl_3/CF_3$-COOD) δ 182.51, 163.40, 160.65, 155.82, 155.68, 146.66, 137.30, 133.10(2C), 129.38, 129.27(2C), 125.98, 125.95, 122.21, 119.97, 119.25, 117.94, 106.80, 94.23; HRMS (ESI) calcd for $C_{20}H_9O_4NBr$ $[M-H]^-$:405.9720 found 405.9724.

*4.4.8. 2-(4-chlorophenyl)-5-hydroxy-6H-xantheno [4, 3-d] oxazol-6-one (**11**)*

Yellow solid (53% yield). Mp 271–273 °C; IR (KBr): 3034, 2922, 1659, 1633, 1611, 1578, 1484, 1470, 1451, 1406, 1388, 1333, 1282,1258, 1217, 1161, 1140, 1091, 1042, 1011, 975, 918, 901, 833, 764, 751, 684, 663, 648 cm^{-1}; ^1H NMR (500 MHz, $CDCl_3$) δ 13.07 (s, 1H), 8.37 (dd, J = 8.0, 1.6 Hz, 1H), 8.22 (d, J = 8.5 Hz, 2H), 7.82 (td, J = 7.6, 6.8, 1.6 Hz, 1H), 7.75 (d, J = 8.4 Hz, 1H), 7.53 (d, J = 8.5 Hz, 2H), 7.50–7.46 (m, 1H), 7.01 (s, 1H); ^{13}C NMR (101 MHz, $CDCl_3/CF_3COOD$) δ 182.34, 163.07, 160.64, 155.94, 155.65, 146.82, 140.23, 137.03, 130.01(2C), 129.19(2C), 126.05, 125.77, 122.40, 120.14, 120.05, 117.96, 106.73, 94.09; HRMS (EI) calcd for $C_{20}H_{10}O_4NCl$ $[M^+]$: m/z = 363.0293 found 363.0281.

*4.4.9. 2-(4-fluorophenyl)-5-hydroxy-6H-xantheno [4, 3-d] oxazol-6-one (**12**)*

Yellow solid (59% yield). Mp 265–267 °C; IR (KBr): 3423, 3049, 2926, 1657, 1635, 1609, 1578, 1472, 1453, 1416, 1389, 1335, 1228, 1161, 1141, 1099, 1041, 1010, 976, 901, 812, 784, 760, 748, 729, 640, 611 cm^{-1}; ^1HNMR (400 MHz, $CDCl_3$) δ 13.11 (s, 1H), 8.36 (dd, J = 8.0, 1.7 Hz, 1H), 8.28 (dd, J = 8.8, 5.2 Hz, 2H), 7.83 (ddd, J = 8.7, 7.0, 1.7 Hz, 1H), 7.75 (d, J = 8.4 Hz, 1H), 7.48 (ddd, J = 8.1, 7.0, 1.1 Hz, 1H), 7.23 (d, J = 8.6 Hz, 2H), 7.01 (s, 1H); ^{13}C NMR (101 MHz, $CDCl_3/CF_3COOD$) δ 182.79, 168.08, 165.51, 162.02 (d, J = 259.0 Hz), 156.02, 155.98, 146.75, 137.69, 130.87 (d, J = 9.6 Hz), 119.29(d, J = 2.92 Hz),126.36(2C), 120.35, 118.82, 118.30, 117.27 (d, J = 22.9 Hz,107.22, 94.62; HRMS (ESI) calcd for $C_{20}H_9O_4NF$ $[M-H]^-$:346.0521 found 346.0522.

*4.4.10. 2-(2-fluorophenyl)-5-hydroxy-6H-xantheno [4, 3-d] oxazol-6-one (**13**)*

Yellow solid (56% yield). Mp 264–266 °C; IR (KBr): 3074, 2799, 1657, 1631, 1610, 1577, 1471, 1450, 1391, 1336, 1282, 1260, 1222, 1158, 1143, 1098, 1057, 1025, 975, 901, 864, 814, 787, 764, 748, 688, 672, 648, 611 cm^{-1}; ^1HNMR (400 MHz, $CDCl_3$) δ 13.13 (s, 1H), 8.36 (d, J = 7.8 Hz, 1H), 8.26 (t, J = 7.5 Hz, 1H), 7.83 (dd, J = 8.6, 6.8 Hz, 1H), 7.76 (d, J = 8.4 Hz, 1H), 7.55 (q, J = 7.3 Hz, 1H), 7.48 (t, J = 7.5 Hz, 1H), 7.33 (dd, J = 16.6, 8.8 Hz, 2H), 7.04 (s, 1H); ^{13}C NMR (101 MHz, $CDCl_3/CF_3COOD$) δ 183.21, 161.52 (d, J = 260.0 Hz), 161.43, 160.60 (d, J = 4.3 Hz), 156.38, 156.24, 147.60, 137.90, 136.35 (d, J = 9.2 Hz), 130.98, 126.70, 126.59, 125.94 (d, J = 3.7 Hz), 120.73, 120.28, 118.61, 118.02 (d, J = 21.1 Hz), 113.01 (d, J = 10.9 Hz), 107.51, 94.82; HRMS (ESI) calcd for $C_{20}H_9O_4NF$ $[M-H]^-$:346.0521 found 346.0520.

*4.4.11. 2-(3-fluorophenyl)-5-hydroxy-6H-xantheno [4, 3-d] oxazol-6-one (**14**)*

Yellow solid (44% yield). Mp 268–270 °C; IR (KBr): 3428, 3075, 2961, 2921, 1658, 1632, 1610, 1577, 1472, 1450, 1392, 1334, 1282, 1259, 1221, 1144, 1102, 1024, 975, 865, 812, 764, 744, 687, 647, 609, 526 cm^{-1}; ^1H NMR (600 MHz, $CDCl_3$) δ 13.14 (s, 1H), 8.36 (dd, J = 7.9, 1.6 Hz, 1H), 8.07 (dt, J = 7.7, 1.2 Hz, 1H), 7.98 (dt, J = 9.4, 2.0 Hz, 1H), 7.84 (ddd, J = 8.6, 7.0, 1.7 Hz, 1H), 7.77 (dd, J = 8.4, 1.1 Hz, 1H), 7.53 (td, J = 8.0, 5.5 Hz, 1H), 7.49 (ddd, J = 8.1, 7.0, 1.1 Hz, 1H), 7.26 (dd, J = 16.6, 2.7 Hz, 1H), 7.03 (s, 1H). ^{13}C NMR (101 MHz, $CDCl_3/CF_3COOD$) δ 186.24, 167.21 (d, J = 248.6 Hz), 166.52 (d, J = 3.3 Hz), 165.16, 160.38, 159.85, 151.39, 140.77, 135.50 (d, J = 8.1 Hz), 131.03 (d, J = 8.6 Hz), 130.36, 129.70, 127.82 (d, J = 3.4 Hz), 125.33, 124.68, 124.19 (d, J = 21.3 Hz), 122.23, 119.04 (d, J = 24.5 Hz), 110.91, 98.07; HRMS (ESI) calcd for $C_{20}H_9O_4NF$ $[M-H]^-$:346.0521 found 346.0522.

*4.4.12. 5-hydroxy-2-(2, 4, 6-trifluorophenyl)-6H-xantheno[4,3-d]-oxaz-ol-6-one(**15**)*

Yellow solid (57% yield). Mp 275–277 °C; IR (KBr): 3081, 2929, 1749, 1658, 1613, 1579, 1475, 1392, 1358, 1281, 1251, 1226, 1180, 1133, 1042, 974, 924, 825, 809, 761, 747, 678, 625, 637, 615 cm^{-1}; ^1H NMR (400 MHz, $CDCl_3$) δ 13.14 (s, 1H), 8.37 (dd, J = 8.0, 1.7 Hz, 1H), 7.86–7.80 (m, 1H), 7.75 (d, J = 8.4 Hz, 1H), 7.49 (t, J = 7.5 Hz, 1H), 7.04 (s, 1H), 6.91 (t, J = 8.7 Hz, 2H); ^{13}C NMR (101 MHz, $CDCl_3/CF_3COOD$) δ 186.51, 170.93 (t, J = 15.5 Hz), 168.36 (t, J = 15.4 Hz), 167.35 (dd, J = 15.4, 7.4 Hz), 165.15, 160.32, 159.88, 159.05, 151.58, 141.10, 130.36, 129.95, 124.74, 124.55, 122.27, 110.98, 106.26 (td, J = 25.8, 4.1 Hz), 98.27; HRMS (ESI) calcd for $C_{20}H_7O_4NF_3$ $[M-H]^-$:382.0332 found 382.0332.

*4.4.13. 5-hydroxy-2-(4-methoxyphenyl)-6H-xantheno [4, 3-d] oxazol-6-one (**16**)*

Yellow solid (59% yield). Mp 247–248 °C; IR (KBr): 3004, 2942, 2836, 1659, 1610, 1578, 1504, 1473, 1450, 1421, 1389, 1335, 1282, 1257, 1228, 1214, 1166, 1140, 1095, 1046, 1024, 975, 915, 861, 784, 760, 747, 637, 608 cm^{-1}; ^1H NMR (400 MHz, $CDCl_3$) δ 13.07 (s, 1H), 8.33 (dd, J = 7.9, 1.6 Hz, 1H), 8.19 (d, J = 8.8 Hz, 1H), 7.80 (ddd, J = 8.6, 7.0, 1.7 Hz, 1H), 7.74 (d, J = 8.4 Hz, 1H), 7.46 (t, J = 7.2 Hz, 1H), 7.02 (d, J = 8.8 Hz, 2H), 6.98 (s, 1H), 3.90 (s, 3H); ^{13}C NMR (101 MHz, $CDCl_3$) δ 181.86, 162.80, 162.51, 160.42, 156.73,

155.75, 147.07, 135.60, 129.38(2C), 126.10, 124.73, 123.06, 120.82, 118.81, 118.21, 114.43(2C), 106.31, 93.52, 55.50; HRMS (ESI) calcd for $C_{21}H_{12}O_5N$ $[M-H]^-$:358.0721 found 358.0723.

4.5. Synthesis of 5-hydroxy-2-(4-hydroxyphenyl)-6H-xantheno [4, 3-d] oxazol-6- one (**17**)

Compound **16** was dissolved in anhydrous CH_2Cl_2 (10.0 mL) and cooled to −8.0 °C under N_2, then BBr_3 (2.0 mL, 1.0 M in CH_2Cl_2, 2.0 mmol) was added dropwise. The mixture was warmed to room temperature and stirred for 24 h, H_2O was added and the resulting mixture extracted with CH_2Cl_2, (3 × 25 mL). The combined CH_2Cl_2 extracts were washed with brine, dried (Na_2SO_4), and concentrated under vacuum, The remaining material was purified by column chromatography (acetone - petroleum ether, 1:2) to produce compound **17.** Yellow solid (81% yield). Mp 268–270 °C; IR (KBr): 3326, 3073, 2925, 1657, 1611, 1573, 1509, 1471, 1452, 1393, 1334, 1284, 1257, 1229, 1141, 1112, 1097, 1042, 976, 900, 830, 762, 747 cm^{-1}; ^1H NMR (400 MHz, DMSO-d_6) δ 12.99 (s, 1H), 10.37 (s, 1H), 8.24 (dd, J = 7.9, 1.7 Hz, 1H), 8.02 (d, J = 8.7 Hz, 2H), 7.96 (ddd, J = 8.6, 7.1, 1.7 Hz, 1H), 7.85 (d, J = 8.4 Hz, 1H), 7.56 (t, J = 7.5 Hz, 1H), 7.20 (s, 1H), 6.96 (d, J = 8.8 Hz, 2H); ^{13}CNMR (101 MHz, DMSO-d_6) δ 181.64, 162.64, 161.46, 159.74, 156.45, 155.47, 146.67, 136.75, 129.60(2C), 125.87, 125.50, 122.90, 120.38, 118.48, 116.81, 116.55(2C), 106.01, 93.72; HRMS (ESI) calcd for $C_{20}H_{10}O_5N$ $[M-H]^-$:344.0564 found 344.0566.

4.6. Synthesis of 2-(4-aminophenyl)-5-hydroxy-6H-xantheno [4, 3-d] oxazol-6-one (**18**)

To a solution of **8** (127 mg) in acetone (25.0 mL), Pd-C (20 mg) was added as catalyst and hydrogenation was carried out at 1 bar for 12 h at 40 °C. The resulting suspension was filtered and concentrated under reduced pressure to obtain crude products which were recrystallized from ethyl acetate to yield pure product **18** as a yellow solid (106 mg, 86%). Mp 231–233 °C; IR (KBr): 3478, 3350, 3217, 2924, 1656, 1608, 1576, 1503, 1471, 1453, 1390, 1332, 1283, 1263, 1229, 1176, 1159, 1139, 1097, 1043, 1007, 975, 900, 822, 785, 761, 749, 699, 682, 643 cm^{-1}; ^1H NMR (400 MHz, DMSO-d_6) δ 12.97 (s, 1H), 8.25 (d, J = 7.9 Hz, 1H), 7.96 (t, J = 7.6 Hz, 1H), 7.86–7.83 (m, 3H), 7.56 (t, J = 7.6 Hz, 1H), 7.17 (s, 1H), 6.69 (d, J = 8.3 Hz, 2H), 6.04 (s, 2H); ^{13}C NMR (101 MHz, DMSO-d_6) δ 181.86, 163.70, 159.44, 156.55, 155.67, 153.15, 146.45, 136.86, 129.38(2C), 126.02, 125.56, 123.29, 120.54, 118.60, 114.06(2C), 112.38, 106.07, 93.77; HRMS (ESI) calcd for $C_{20}H_{11}O_4N_2$ $[M-H]^-$:343.0713 found 343.0723.

4.7. General procedure for the preparation of **19–21**

A mixture of compounds **6, 11, 16**(1.0 equiv.), K_2CO_3 (20.0 equiv.) and CH_3I (24.0 equiv.) in acetone (5.0 mL) was stirred at room temperature for 24 h. The reaction mixture was added to 25.0 mL of 2.0 M HCl and extracted with EtOAc (3 × 25 mL). The combined organic layers were dried, filtered and evaporated under vacuum. The crude product was purified by column chromatography (acetone-chloroform, 1:100) to produce compounds **19**–**21** (88–92% yield).

4.7.1. 5-methoxy-2-phenyl-6H-xantheno [4, 3-d] oxazol-6-one (**19**)

White solid (91% yield). Mp 272–274 °C; IR (KBr): 3485, 3070, 2949, 1658, 1635, 1609, 1582, 1466, 1425, 1376, 1303, 1193, 1170, 1134, 1225, 1103, 1046, 1028, 1011, 920, 897, 833, 726, 709, 665, 615 cm^{-1}; ^{1}HNMR (400 MHz, $CDCl_3$) δ 8.36 (dd, J = 7.8, 1.5 Hz, 1H), 8.28 (dd, J = 7.2, 2.7 Hz, 2H), 7.77–7.65 (m, 2H), 7.56 (d, J = 2.0 Hz, 2H), 7.55 (d, J = 1.9 Hz, 1H), 7.41 (ddd, J = 8.1, 6.3, 1.9 Hz, 1H), 7.06 (s, 1H), 4.10 (s, 3H); ^{13}CNMR (101 MHz, $CDCl_3$) δ 175.77, 162.69, 159.91, 155.16, 154.64, 149.57, 134.19, 131.69, 128.99(2C), 127.50(2C), 126.89, 126.44, 124.58, 124.52, 123.31, 117.63, 110.18, 89.70, 57.00; HRMS (ESI) calcd for $C_{21}H_{14}NO_4$ $[M+H]^+$:344.0933 found 344.0923.

4.7.2. 5-methoxy-2-(4-methoxyphenyl)-6H-xantheno [4, 3-d] oxazol-6-one (**20**)

White solid (92% yield). Mp 233–235 °C; IR (KBr): 3483, 3067, 2949, 1659, 1635, 1609, 1586, 1466, 1421, 1398, 1376, 1333, 1302, 1262, 1225, 1197, 1134, 1160, 1103, 1069, 1044, 109, 921, 894, 826, 800, 749, 723, 685, 644, 612 cm^{-1}; ^{1}HNMR (400 MHz, $CDCl_3$) δ 8.35 (dd, J = 7.7, 1.4 Hz, 1H), 8.22–8.18 (m, 2H), 7.73–7.66 (m, 2H), 7.39 (ddd, J = 8.1, 6.4, 1.8 Hz, 1H), 7.04 (d, J = 8.9 Hz, 2H), 7.03 (s, 1H), 4.08 (s, 3H), 3.90 (s, 3H). ^{13}C NMR (101 MHz, $CDCl_3$) δ 171.06, 158.08, 157.68, 154.77, 150.29, 149.89, 144.48, 129.38, 124.53(2C), 122.10, 119.86, 119.67, 118.51, 114.16, 112.85, 109.66(2C), 105.26, 84.93, 52.21, 50.73; HRMS (ESI) calcd for $C_{22}H_{16}O_5N$ $[M+H]^+$:374.1023 found 374.1014.

4.7.3. 2-(4-chlorophenyl)-5-methoxy-6H-xantheno [4, 3-d] oxazol-6-one (**21**)

White solid (88% yield). Mp 248–250 °C; IR (KBr): 3481, 3064, 2941, 1657, 1625, 1607, 1583, 1464, 1426, 1376, 1324, 1191, 1173, 1134, 1222, 1112, 1046, 1025, 1011, 921, 899, 823, 724, 704, 661, 616 cm^{-1}; ^{1}HNMR (400 MHz, $CDCl_3$) δ 8.35 (dd, J = 8.0, 1.6 Hz, 1H), 8.20 (d, J = 8.3 Hz, 2H), 7.71 (t, J = 7.6 Hz, 1H), 7.67 (d, J = 8.3 Hz, 1H), 7.52 (d, J = 8.3 Hz, 2H), 7.40 (t, J = 7.4 Hz, 1H), 7.03 (s, 1H), 4.09 (s, 3H). ^{13}CNMR (101 MHz, $CDCl_3$) δ 175.69, 161.70, 160.09, 155.14, 154.60, 149.60, 137.97, 134.25, 129.39 (2C), 128.71(2C), 126.91, 124.92, 124.60, 124.52, 123.31, 117.59, 110.28, 89.65, 57.03; HRMS (ESI) calcd for $C_{21}H_{13}NO_4Cl$ $[M+H]^+$:378.0539 found 378.0533.

4.8. Biological studies

4.8.1. α-glucosidase inhibitory assays

The inhibitory activities of compounds **1b**, **2**–**16** were measured by using the methods similar to those described previously.[14–19] Typically, α-glucosidase activity was assayed in 50 mM phosphate buffer (pH 6.8) containing 5% v/v DMSO, and PNP glycoside was used as a substrate. The inhibitors were pre-incubated with the enzyme at 37 °C for 30 min, and then the substrate was added. The enzymatic reaction was carried out at 37 °C for 60 s and monitored spectrophotometrically by measuring the absorbance at 400 nm. The assay was performed in triplicate with five different inhibitor concentrations around the IC_{50} values that were roughly estimated in the first round of experiments, and the mean values were taken.

4.8.2. Kinetics of enzyme inhibition

The inhibition types of the selected compounds were determined from Lineweavere-Burk plots, using the methods similar to those reported previously.[18,34,35] Typically, two different concentrations of each compound around the IC_{50} values were chosen. With each concentration, α-glucosidase activity was assayed by varying the concentration of PNP glycoside. The enzyme reaction was performed using the conditions described above. The mixtures of the enzyme and the inhibitor were dissolved in 50 mM phosphate buffer (pH 6.8) containing 5% v/v DMSO, pre-incubated at 37 °C for 30 min, and then the substrate was added. The enzyme reaction was carried out at 37 °C for 60 s, and monitored spectrophotometrically by measuring the absorbance at 400 nm. Inhibition types and *Ki* values of the inhibitors were determined using double-reciprocal plots.

5. Molecular docking studies

The model of α-glucosidase for docking studies, obtained from the SWISS-MODEL Repository,[36] was constructed by homology modelling using oligo-1,6-glucosidase from Saccharomyces cerevisiae (PDB: 3AXH) as the template (sequence identity: 72.51%). Gasteiger partial charges were assigned and non-polar hydrogen atoms were merged using AutoDock Tools.[38,39] The ligands were structured and optimized using ChemBioDraw Ultra 12.0, ChemBio3D Ultra 12.0 and Gaussian 09 W,[40] followed by format transformation to PDBQT files using Autodock Tools. The docking studies were run using AutodockVina[41] and the results of the docking procedures were visualized using AutoDock Tools.

Acknowledgments

We are thankful to Prof. Wen-Hua Chen (Southern Medical University) and Prof. Zhuofeng Ke (Sun Yat-sen University) for their helpful discussions and comments. We are thankful to Prof. Jeff Lawton (Eastern University) for his generously providing us editorial assistance. This work was supported by the National Natural Science Foundation of China (Nos. 21272290 and J1103305) and the Fund for Undergraduate Innovation Program from Sun Yat-sen University.

A. Supplementary data

Supplementary data associated with this article can be found, in the online version, at https://doi.org/10.1016/j.bmc.2018.05.008.

References

1. Hirsh AJ, Yao SYM, Young JD, Cheeseman CI. Inhibition of glucose absorption in the rat jejunum: a novel action of. *Gastroenterology*. 1997;113:205–211.
2. Van de Laar A. Alpha-glucosidase inhibitors in the early treatment of type 2 diabetes. *Vasc Health Risk Manage*. 2008;4:1189–1195.
3. Rhabasa-Lhoret R, Chiasson JL, Defronzo RA, Ferrannini E, Keen H, Zimmei P. *International textbook of diabetes mellitus*, Vol. 1. UK: John Wiley; 2004.
4. Bhat M, Zinjarde SS, Bhargava SY, Kumar AR, Joshi BN. Antidiabetic Indian plants: a good source of potent amylase inhibitors. *Evi. Based Complement Alternate Med.*. 2011;2011(1741-427X):81020.
5. Meneilly GS, Ryan EA, Radziuk J, Lau DCW, Morais J. Effect of acarbose on insulin sensitivity in elderly patients with diabetes. *Diabetes Care*. 2000;23:1162–1167.
6. Scott LJ, Spencer CM. Miglitol. *Drugs*. 2000;59:521–549.
7. Davis SN, Granner DK. *The Pharmacological basis of therapeutics*. 9th ed. New York: McGraw-Hill; 1996. 1487–1517.
8. Gallienne E, Gefflaut T, Bolte J, Lemaire M. Synthesis of new nitrogen analogues of salacinol and deoxynojirimycin and their evaluation as glycosidase inhibitors. *J Org Chem*. 2006;71:894–902.
9. Groopman JE. Current advances in the diagnosis and treatment of AIDS: an introduction. *Rev Infect Dis*. 1990;12:908–911.
10. Sou S, Takahashi H, Yamasaki R, Kagechika H, Endo Y, Hashimoto Y. ALPHA.-glucosidase inhibitors with a 4,5,6,7-tetrachlorophthalimide skeleton pendanted with a cycloalkyl or dicarba-closo-dodecaborane Group. *Chem Pharm Bull (Tokyo)*. 2001;49:791–793.
11. Khan M, Yousaf M, Wadood A, et al. Discovery of novel oxindole derivatives as potent α-glucosidase inhibitors. *Bioorg Med Chem*. 2014;22:1195–1200.
12. Negi JS, Bisht VK, Singh P, Rawat MSM, Joshi GP. Naturally occurring xanthones: chemistry and biology. *J Appl Chem*. 2013;2013:1–9.
13. Pedraza-Chaverri J, Cárdenas-Rodríguez N, Orozco-Ibarra M, Pérez-Rojas JM. Medicinal properties of mangosteen (Garcinia mangostana). *Food Chem Toxicol*. 2008;46:3227–3239.
14. Liu Y, Zou L, Ma L, Chen W-H, Wang B, Xu Z-L. Synthesis and pharmacological activities of xanthone derivatives as α-glucosidase inhibitors. *Bioorg Med Chem*. 2006;14:5683–5690.
15. Liu Y, Ma L, Chen W-H, Wang B, Xu Z-L. Synthesis of xanthone derivatives with extended π-systems as α-glucosidase inhibitors: insight into the probable binding mode. *Bioorg Med Chem*. 2007;15:2810–2814.
16. Liu Y, Ke Z, Cui J-F, Chen W-H, Ma L, Wang B. Synthesis, inhibitory activities, and QSAR study of xanthone derivatives as α-glucosidase inhibitors. *Bioorg Med Chem*. 2008;16:7185–7192.
17. Li G-L, He J-Y, Zhang A, Wan Y, Wang B, Chen W-H. Toward potent α-glucosidase inhibitors based on xanthones: a closer look into the structure-activity correlations. *Eur J Med Chem*. 2011;46:4050–4055.
18. Liu Y, Ma L, Chen W-H, Park H, Ke Z, Wang B. Binding mechanism and synergetic effects of xanthone derivatives as noncompetitive alpha-glucosidase inhibitors: a theoretical and experimental study. *J Phys Chem B*. 2013;117:13464–13471.
19. Li G-L, Cai C-Y, He J-Y, et al. Synthesis of 3-acyloxyxanthone derivatives as α-glucosidase inhibitors: a further insight into the 3-substituents' effect. *Bioorg Med Chem*. 2016;24:1431–1438.
20. Verma NK, Singh SP, Rai PK, Tripathi AK. Scholars research library. *Der Pharm Lett*. 2014;6:283–288.
21. Boulogne I, Petit P, Ozier-Lafontaine H, Desfontaines L, Loranger-Merciris G. Insecticidal and antifungal chemicals produced by plants: a review. *Environ Chem Lett*. 2012;10:325–347.
22. El-All ASA, Osman SA, Roaiah HMF. Potent anticancer and antimicrobial activities of pyrazole, oxazole and pyridine derivatives containing 1,2,4-triazine moiety. *Med Chem Res*. 2015;24:1–12.
23. Liu X-H, Lv P-C, Xue J-Y, Song B-A, Zhu H-L. Novel 2,4,5-trisubstituted oxazole derivatives: synthesis and antiproliferative activity. *Eur J Med Chem*. 2009;44:3930–3935.
24. Moraski GC, Chang M, Villegas-Estrada A, Franzblau SG, Möllmann U, Miller MJ. Structure-activity relationship of new anti-tuberculosis agents derived from oxazoline and oxazole benzyl esters. *Eur J Med Chem*. 2010;45:1703–1716.
25. White RLJ, Wessels FL, Schwan TJ. ChemInform abstract: 1-(((5-(Substituted Phenyl)-2-oxazolyl)methylene)amino)-2,4-imidazolidinediones, a New Class of Skeletal Muscle Relaxants. *J Med Chem*. 1987;30:263–266.
26. Zhang F, Chapman KT, Schleif WA, et al. The design, synthesis and evaluation of novel HIV-1 protease inhibitors with high potency against PI-resistant viral strains. *Bioorg Med Chem Lett*. 2003;13:2573–2576.
27. Conti P, Dallanoce C, De Amici M, De Micheli C, Klotz K. Synthesis of new-isoxazoline derivatives and their pharmacological characterization as-adrenergic receptor antagonists. *Bioorg Med Chem*. 1998;6:401–408.
28. Sittisombut C, Costes N, Michel S, et al. Synthesis and cytotoxic activity of benzopyranoxanthone analogues of benzo[b]acronycine and psorospermine. *Chem Pharm Bull*. 2001;49:675–679.
29. Pillai RKM, Naiksatam P, Johnson F, et al. 1,3-Dihydroxy-9H-xanthones and 1,3-Dihydroxy-9H-xanthenes. *J Org Chem*. 1986;51:717–723.
30. Gao H. Kawabata J. alpha-Glucosidase inhibition of 6-hydroxyflavones. Part 3: synthesis and evaluation of 2,3,4-trihydroxybenzoyl-containing flavonoid analogs and 6-aminoflavones as alpha-glucosidase inhibitor. *Bioorg Med Chem*. 2005;13:1661–1671.
31. Fekner T, Gallucci J, Chan MK. Ruffling-induced chirality: synthesis, metalation, and optical resolution of highly nonplanar, cyclic, Benzimidazole-based ligands. *J Am Chem Soc*. 2004;126:223–236.
32. Sugimoto N, Kawasaki Y, Sato KM, et al. Structure of acid-stable carmine. *J Food Hyg Soc Jpn*. 2002;43:18–23.
33. Zielske AG. (Tosyloxy) anthraquinones: versatile synthones for the preparation of various aminoanthraquinones. *J Org Chem*. 1987;52:1305–1309.
34. Wang Y, Ma L, Pang C, Huang M, Huang Z, Gu L. Synergetic inhibition of genistein and D-glucose on α-glucosidase. *Bioorg Med Chem Lett*. 2004;14:2947–2950.
35. Wang Y, Ma L, Li Z, Du Z-Y. Synergetic inhibition of metal ions and genistein on α-glucosidase. *FEBS Lett*. 2004;576:46–50.
36. Bienert S, Waterhouse A, de Beer TA, et al. The SWISS-MODEL Repository – new features and functionality. *Nucleic Acids Res*. 2017;45:D313–D319.
37. Adisakwattana S, Charoenlertkul P, Yibchok-Anun S. A-glucosidase inhibitory activity of cyanidin-3-galactoside and synergistic effect with acarbose. *J Enzyme Inhib Med Chem*. 2009;24:65–69.
38. Sanner MF. Python: a programming language for software integration and development. *J Mol Graph Model*. 1999;17:57–61.
39. Morris GM, Huey R, Lindstrom W, et al. Software news and updates AutoDock4 and AutoDockTools4: automated docking with selective receptor flexibility. *J Comput Chem*. 2009;16:2785–2791.
40. Frisch MJ, Trucks GW, Schlegel HB, et al. *Gaussian 09, Revision A.02*. Wallingford CT: Gaussian Inc; 2009.
41. Trott O, Olson AJ. AutoDock Vina: improving the speed and accuracy of docking with a new scoring function, efficient optimization, and multithreading. *J Comput Chem*. 2009;31:455–461.